Restoration of Missing Data in Limited Angle Tomography Based on Consistency Conditions

Yixing Huang*, Oliver Taubmann*†, Xiaolin Huang*‡,
Joachim Hornegger*†, Guenter Lauritsch¶ and Andreas Maier*†
*Pattern Recognition Lab, Friedrich-Alexander-University Erlangen-Nuremberg, Erlangen, Germany
†Erlangen Graduate School in Advanced Optical Technologies (SAOT), Erlangen, Germany
‡Institute of Image Processing and Pattern Recognition, Shanghai Jiao Tong University, Shanghai, China
¶Siemens Healthcare GmbH, Forchheim, Germany

Email: yixing.yh.huang@fau.de

***Abstract*—In limited angle tomography, only a limited angular range of data is acquired and consequently a double wedge-shaped region in the frequency domain representation of the imaged object is missing. Hence, streak artifacts occur. To restore the missing data, we perform a regression and an image fusion in sinogram domain and frequency domain, respectively. We first convert the sinogram restoration problem into a regression problem based on the Helgason-Ludwig consistency conditions. Due to the severe ill-posedness of the problem, regression only partially recovers the correct frequency components, especially lower frequency components, and will introduce erroneous ones, particularly higher frequencies. Bilateral filtering is utilized to retain the most prominent high frequency components and suppress erroneous ones. A fusion of the filtered image and the image reconstructed from the limited angle sinogram is performed afterwards in the frequency domain. The proposed method is evaluated on the Shepp-Logan phantom, for which the root-mean-square error of the reconstructed image decreases from 310 HU to 136 HU.**

I. Introduction

In computed tomography (CT), image reconstruction from data acquired in an insufficient angular range is called limited angle tomography. It arises when the gantry rotation of a CT system is restricted by other system parts or external obstacles. Because of missing data, artifacts, typically in the form of streak artifacts, will occur in the reconstructed images.

The ill-posedness of the limited angle tomography problem has been well investigated [1], [2]. Iterative reconstruction algorithms can incorporate prior information. In particular, iterative reconstruction algorithms with total variation (TV) regularization, which exploits sparsity in the image gradient domain, have become popular in limited angle tomography [3]–[6]. However, the high computational cost of iterative algorithms restrains their clinical applications. Deep learning techniques can learn compensation weights [7] to correct the mass loss in a filtered back-projection (FBP) reconstruction while keeping the same computational complexity [8].

An alternative approach is to restore the missing projection data based on data consistency conditions. Many consistency conditions have been explored, e.g., epipolar consistency in cone-beam CT [9], John's equation [10], and the polynomial behavior of truncated data [11]. The Helgason-Ludwig consistency conditions (HLCC) [12], [13] are the most well-known and they are necessary and sufficient for a transform to be a Radon transform [14]. Louis reformulated the sinogram extrapolation problem into a system of linear equations based on HLCC such that an approximate sinogram can be estimated [15]. Willsky et al. and Kudo et al. also proposed to use HLCC for limited angle reconstruction [16], [17].

In this paper, we propose a regression and fusion method to restore the missing data for limited angle tomography. Numerical experiments on the Shepp-Logan phantom demonstrate that the proposed method can reduce streak artifacts well.

II. Method and materials

A. Background theory

The parallel-beam sinogram of a 2-D object $f(x, y)$ is denoted by $p(s, \theta)$, where θ is the rotation angle and s is the detector index with the assumption $-1 \leq s \leq 1$. We define the nth order moment curve of $p(s, \theta)$ as,

$$a_n(\theta) = \int_{-1}^{1} p(s, \theta) T_n(s) \mathrm{d}s, \tag{1}$$

where $T_n(s) = s^n$. The Fourier transform of the moment curve is,

$$b_{n,m} = \frac{1}{2\pi} \int_0^{2\pi} a_n(\theta) e^{-im\theta} \mathrm{d}\theta. \tag{2}$$

HLCC [12], [13] can be expressed as,

$$b_{n,m} = 0, \quad |m| > n \text{ or } n + m \text{ is odd}. \tag{3}$$

$p(s, \theta)$ can be conveniently restored from $a_n(\theta)$ when $T_n(s)$ is replaced by orthogonal polynomials. In this paper, we use the Chebyshev polynomial of the second kind,

$$U_n(s) = \frac{\sin((n+1)\arccos(s))}{\sqrt{1-s^2}}. \tag{4}$$

$U_n(s)$ is a family of orthogonal polynomials at domain [-1, 1] with the weight $W(s) = (1-s^2)^{1/2}$. Thus, an approximate sinogram can be restored by the inverse Chebyshev transform,

$$p_{n_r}(s, \theta) = \frac{2}{\pi} \sum_{n=0}^{n_r} a_n(\theta)(W(s) \cdot U_n(s)), \tag{5}$$

DOI: 10.12059/Fully3D.2017-11-3201006

where n_r stands for the number of orders used.

The Fourier transform of $W(s) \cdot U_n(s)$ is computed as,

$$\mathcal{F}(W(s) \cdot U_n(s))(w) = \pi(J'_{n+2}(iw) - J'_n(iw)), \quad (6)$$

where $\mathcal{F}$ is the Fourier transform operator and $J'_n(z)$ is the modified Bessel function of order n [18]. Because $J'_n(z)$ rapidly tends to zero when $|z|$ becomes less than n, $W(s) \cdot U_n(s)$ can be regarded as a high-pass filter with an cut-off frequency denoted by $w_{c,n}$. Therefore, only a circular area with radius w_{c,n_r} is restored completely in the Fourier representation of the imaged object if we use $p_{n_r}(s,\theta)$ for reconstruction, since the missing polynomials of orders higher than n_r only contribute to the frequency range above w_{c,n_r}.

B. Regression method for sinogram restoration

We denote the projection angles as $\boldsymbol{\theta} = [\theta_0, \theta_1, ..., \theta_{N-1}]^\top$ where $0 \leq \theta_k < \theta_{\max}, k = 0, 1, ..., N-1$, $\theta_{\max}$ is the maximum scanned angle, and N is the total number of acquired projections. We further denote the missing angular range as $\Phi = \pi - \theta_{\max}$. Then, N samples on the moment curve of order n are available, denoted by $\boldsymbol{a}_n(\boldsymbol{\theta}) = [a_n(\theta_0), a_n(\theta_1), a_n(\theta_2), ..., a_n(\theta_{N-1})]^\top$. We seek to restore the complete 180° sinogram at the angles $\boldsymbol{\theta}_{\text{comp}} = [0, 1, ..., K-1] \cdot \Delta\theta$ from the acquired samples where $K = \lfloor \pi/\Delta\theta \rfloor$ and $\Delta\theta$ is the angular step.

Due to HLCC, Eq. (2) can also be represented as the following trigonometric Fourier series,

$$a_n(\theta) = c_{n,0} + \sum_{m=1}^{n} (c_{n,m}\cos(m\theta) + d_{n,m}\sin(m\theta)), \quad (7)$$

where $c_{n,0} = b_{n,0}$ and $(c_{n,m} - d_{n,m}i)/2 = b_{n,m}$. Accordingly, $c_{n,m} = 0$ and $d_{n,m} = 0$ when $n+m$ is odd. That is, when n is even, m can be $0, 2, 4, ..., n-2, n$. Thus, $a_n(\theta)$ has $n+1$ unknown coefficients denoted by,

$$\boldsymbol{\beta}_{n,\text{e}} = [c_{n,0}, c_{n,2}, d_{n,2}, c_{n,4}, d_{n,4}, \ldots, c_{n,n}, d_{n,n}]^\top. \quad (8)$$

As a result, we get the linear regression problem,

$$\begin{aligned}&[\mathbf{1}, \cos(2\boldsymbol{\theta}), \sin(2\boldsymbol{\theta}), \cos(4\boldsymbol{\theta}), \sin(4\boldsymbol{\theta}), \ldots,\\ &\cos(n\boldsymbol{\theta}), \sin(n\boldsymbol{\theta})]\boldsymbol{\beta}_{n,\text{e}} = \boldsymbol{a}_n(\boldsymbol{\theta}),\end{aligned} \quad (9)$$

where $\cos(\cdot)$ and $\sin(\cdot)$ are element-wise operators.

When n is odd, we get a similar regression problem with again $n+1$ unknown parameters,

$$\begin{aligned}&[\cos(\boldsymbol{\theta}), \sin(\boldsymbol{\theta}), \cos(3\boldsymbol{\theta}), \sin(3\boldsymbol{\theta}), \ldots,\\ &\cos(n\boldsymbol{\theta}), \sin(n\boldsymbol{\theta})]\boldsymbol{\beta}_{n,\text{o}} = \boldsymbol{a}_n(\boldsymbol{\theta}),\end{aligned} \quad (10)$$

where

$$\boldsymbol{\beta}_{n,\text{o}} = [c_{n,1}, d_{n,1}, c_{n,3}, d_{n,3}, \ldots, c_{n,n}, d_{n,n}]^\top. \quad (11)$$

For each case, the regression problem can be written as,

$$\boldsymbol{X}_n(\boldsymbol{\theta})\boldsymbol{\beta}_n = \boldsymbol{a}_n(\boldsymbol{\theta}). \quad (12)$$

With an estimate $\hat{\boldsymbol{\beta}}_n$ of parameters $\boldsymbol{\beta}_n$, the complete nth moment curve $\hat{\boldsymbol{a}}_n(\boldsymbol{\theta}_{\text{comp}})$ is obtained as

$$\hat{\boldsymbol{a}}_n(\boldsymbol{\theta}_{\text{comp}}) = \boldsymbol{X}_n(\boldsymbol{\theta}_{\text{comp}})\hat{\boldsymbol{\beta}}_n. \quad (13)$$

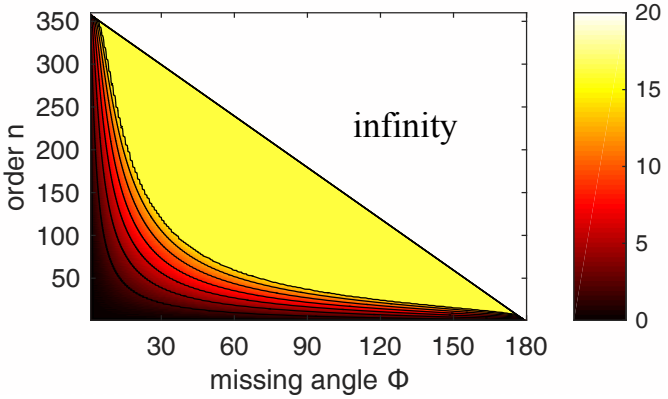

Fig. 1. Condition numbers of $\boldsymbol{X}_n(\boldsymbol{\theta})$ as a function of the order and the missing angular range. The condition numbers are logarithmized as $\log_{10}(\kappa_n)$ and the lines are contours with step size 2.

Then the complete sinogram can be restored using Eq. (5) and the object can be reconstructed.

The conversion of the sinogram restoration problem into the regression problem in Eq. (12) has the following benefits:

(i) $\boldsymbol{\theta}$ can be a partial angular range and it does not have to be uniformly distributed.

(ii) We can investigate its ill-posedness conveniently by computing the condition number of matrix $\boldsymbol{X}_n(\boldsymbol{\theta})$. An example is displayed in Fig. 1. It indicates that when the order n or the missing angular range Φ increases, the condition number increases drastically. When $n \geq N = (180^\circ - \Phi)/\Delta\theta$ (the upper right triangle), $\boldsymbol{X}_n(\boldsymbol{\theta})$ with size $N \times (n+1)$ becomes underdetermined. Therefore, the regression problem (Eq. (12)) for sinogram restoration is ill-posed.

(iii) Various existing algorithms are available to solve ill-posed regression problems. Here we use Lasso regression [19],

$$\boldsymbol{\beta}_n = \arg\min \frac{1}{2}||\boldsymbol{X}_n(\boldsymbol{\theta})\boldsymbol{\beta}_n - \boldsymbol{a}_n(\boldsymbol{\theta})|| + \tau_n||\boldsymbol{\beta}_n||_1, \quad (14)$$

where τ_n is a regularization coefficient. It can be solved by the iterative soft-thresholding algorithm [20].

C. Image fusion in frequency domain

The proposed regression method is applied to restore the complete sinogram $p_{n_r}(s,\theta)$. The image reconstructed from $p_{n_r}(s,\theta)$ is denoted by $f_{\text{HLCC}}(x,y)$. Since the condition number of $\boldsymbol{X}_n(\boldsymbol{\theta})$ increases drastically when n increases, only certain orders of the moment curves are estimated correctly. Let n_c denote the highest order that is still estimated correctly. Then, the frequency components of $f_{\text{HLCC}}(x,y)$ are only correct inside a circular area with radius w_{c,n_c}. Consequently, regression errors in the restored moment curves from order n_c+1 to n_r will introduce artifacts.

To obtain only the most prominent and reliable high frequency components associated with sharp edges and suppress erroneous smaller ones, a strong bilateral filter (BF) [21] is applied to f_{HLCC}. The filtered image is denoted by f_{BF}.

We denote the image reconstructed from the limited angle sinogram by $f_{\text{limited}}(x,y)$ and its 2-D Fourier transform in

polar coordinates by $F_{\text{limited}}(w,\theta)$. The central slice theorem reveals that a double wedge region is missing, i.e.,

$$F_{\text{limited}}(w,\theta)|_{\theta_{\max}\leq\theta<\pi,-\infty<w<\infty} = 0. \tag{15}$$

We only want to use the information contained in f_{BF} to fill in these unobserved regions. For this purpose, we design a double wedge-shaped mask $M(w,\theta)$ in frequency domain where values outside the double wedge zero region are 1. The binary mask $M(w,\theta)$ is smoothed by a Gaussian filter to get a smooth transition at its boundary. Then the following image fusion (Fig. 2) is performed,

$$F_{\text{fused}} = F_{\text{limited}} \cdot M + F_{\text{BF}} \cdot (\mathbf{1} - M), \tag{16}$$

where F_{BF} is the 2-D Fourier transform of f_{BF} and the operators are to be understood element-wise. The fused image f_{fused} can be obtained from F_{fused} afterwards.

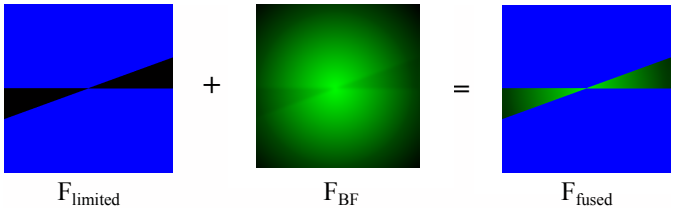

Fig. 2. Illustration of the fusion in frequency domain. The black and blue areas are the missing and measured frequency components respectively. The green frequency components are estimated by HLCC and the bilateral filter where the faded green area might be estimated incorrectly.

D. Experimental setup

To evaluate the performance of our proposed method, a simulation experiment is conducted with the standard high-contrast pixelized Shepp-Logan phantom (Fig. 4(a)). Its image size is 512×512 with an isotropic pixel size of 0.4 mm. The linear attenuation coefficients are between [-1000, 3000] HU.

The limited angle sinogram is simulated with a parallel-beam trajectory using a ray-driven method with a sampling rate of $7.5/\text{mm}$. No noise is simulated. The total scanned angular range is $160°$ and the angular step is $0.5°$. The number of the equal-space detector pixels N_D is 1537 and the detector element size is 0.2 mm.

Empirically, we choose $n_r = 720$ to restore the sinogram. For each order n, the soft-threshold $\tau_n = 0.001 \cdot (1 - n/1000)$ is used and the iteration stops when $||\hat{\boldsymbol{\beta}}_n^{l+1} - \hat{\boldsymbol{\beta}}_n^{l}||_2 / ||\hat{\boldsymbol{\beta}}_n^{l}||_2 < 10^{-4}$ where $\hat{\boldsymbol{\beta}}_n^{l}$ are the estimated parameters at l-th iteration.

The images are reconstructed using FBP with the Ram-Lak kernel. The bilateral filter is characterized by the geometric spread $\sigma_c = 30$ and the photometric spread $\sigma_s = 0.05$ defined on an $\mathcal{N} = 40 \times 40$ neighborhood [21]. The binary mask $M(w,\theta)$ is smoothed by a Gaussian filter with a cutoff frequency at 0.4 Nyquist frequency. The experimental setup is implemented in CONRAD [22].

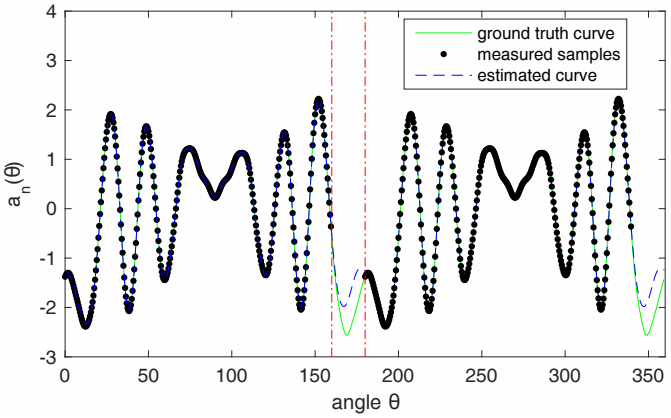

Fig. 3. Plot of curve $\hat{\boldsymbol{a}}_{100}(\boldsymbol{\theta}_{\text{comp}})$ as an example to illustrate the regression. The area in the two red lines is the missing part and the angular range $[180°, 360°)$ is displayed based on $p(s,\theta) = p(-s,\theta+\pi)$.

III. Results And Discussion

The curve of $\hat{\boldsymbol{a}}_{100}(\boldsymbol{\theta}_{\text{comp}})$ is plotted in Fig. 3(a) as an example to illustrate the regression problem. It shows that the estimated moment curve has some deviations to the ground truth moment curve $\boldsymbol{a}_{100}(\boldsymbol{\theta}_{\text{comp}})$, indicating the existence of regression errors.

The reconstructed images and their absolute differences from the ground truth are shown in Fig. 4. Comparing f_{HLCC} with f_{limited}, large streak artifacts are reduced and the shape of the outer boundary is reconstructed better in f_{HLCC}. However, it suffers from artifacts caused by regression errors, which appear as small streaks. Fig. 4(g) reveals that the edge areas in f_{HLCC} also have large errors. This results from the missing high frequency components due to the low number of n_r. Figs. 4(d) demonstrates that the bilateral filter can remove artifacts and partially recover the high contrast edges. With the image fusion, streak artifacts are reduced in f_{fused} while avoiding the introduction of new artifacts due to regression.

IV. Conclusion

In this paper, we propose a regression and fusion method for limited angle tomography to restore missing data. The limited angle sinogram restoration problem is converted into a regression problem based on HLCC. A strong bilateral filter is used to preserve prominent sharp edges and reduce artifacts caused by the regression. Afterwards, a fusion in the frequency domain utilizes the restored frequency components to fill the missing double wedge region. With our proposed method, streak artifacts can be reduced in the final fused image.

Disclaimer: The concepts and information presented in this paper are based on research and are not commercially available.

References

[1] M. E. Davison, "The ill-conditioned nature of the limited angle tomography problem," *SIAM Journal on Applied Mathematics*, vol. 43, no. 2, pp. 428–448, 1983.

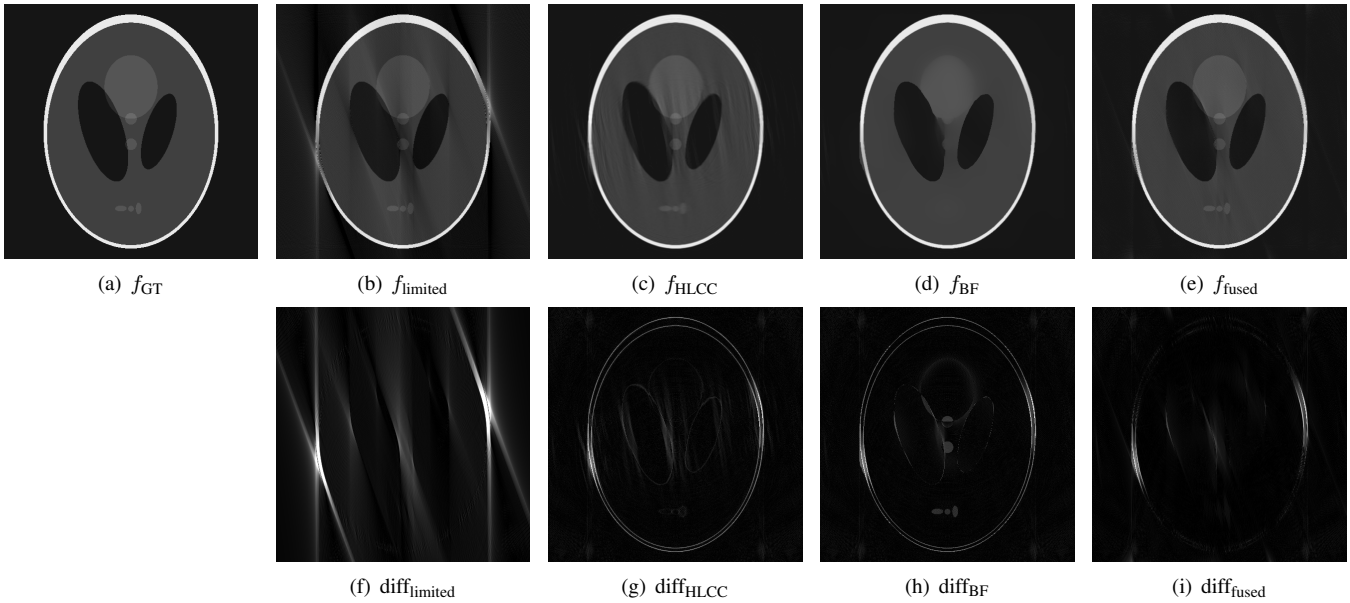

(a) f_{GT} (b) f_{limited} (c) f_{HLCC} (d) f_{BF} (e) f_{fused}

(f) $\text{diff}_{\text{limited}}$ (g) $\text{diff}_{\text{HLCC}}$ (h) diff_{BF} (i) $\text{diff}_{\text{fused}}$

Fig. 4. Reconstructions of the Shepp-Logan phantom and their absolute difference from the ground truth. The root-mean-square errors (RMSEs) for f_{limited}, f_{HLCC}, f_{BF}, and f_{fused} are 310 HU, 189 HU, 178 HU, and 136 HU, respectively. Window: [-1400, 3400] HU and [-1000, 1000] HU for the top row and the middle row images, respectively.

[2] A. K. Louis, "Incomplete data problems in X-ray computerized tomography: I. singular value decomposition of the limited angle transform," *Numerische Mathematik*, vol. 48, no. 3, pp. 251–262, 1986.

[3] E. Y. Sidky and X. Pan, "Image reconstruction in circular cone-beam computed tomography by constrained, total-variation minimization," *Physics in Medicine and Biology*, vol. 53, no. 17, p. 4777, 2008.

[4] L. Ritschl, F. Bergner, C. Fleischmann, and M. Kachelrieß, "Improved total variation-based CT image reconstruction applied to clinical data," *Physics in Medicine and Biology*, vol. 56, no. 6, p. 1545, 2011.

[5] Z. Chen, X. Jin, L. Li, and G. Wang, "A limited-angle CT reconstruction method based on anisotropic TV minimization," *Physics in Medicine and Biology*, vol. 58, no. 7, p. 2119, 2013.

[6] Y. Huang, O. Taubmann, X. Huang, V. Haase, G. Lauritsch, and A. Maier, "A New Scale Space Total Variation Algorithm for Limited Angle Tomography," in *CT-Meeting 2016 Proceedings (The 4th International Meeting on Image Formation in X-Ray Computed Tomography)*, M. Kachelrieß, Ed., 2016, pp. 149–152.

[7] C. Riess, M. Berger, H. Wu, M. Manhart, R. Fahrig, and A. Maier, "TV or not TV? That is the Question," in *Fully 3D Image Reconstruction in Radiology and Nuclear Medicine*, 2013, pp. 341–344.

[8] T. Würfl, F. C. Ghesu, V. Christlein, and A. Maier, "Deep Learning Computed Tomography," in *Medical Image Computing and Computer-Assisted Intervention MICCAI 2016*, Springer, Ed., vol. 3, 2016, pp. 432–440.

[9] A. Aichert, M. Berger, J. Wang, N. Maass, A. Doerfler, J. Hornegger, and A. Maier, "Epipolar consistency in transmission imaging," *IEEE Transactions on Medical Imaging*, vol. 34, no. 10, pp. 1–15, 2015.

[10] S. K. Patch, "Consistency conditions upon 3D CT data and the wave equation," *Physics in Medicine and Biology*, vol. 47, no. 15, p. 2637, 2002.

[11] R. Clackdoyle and L. Desbat, "Data consistency conditions for truncated fanbeam and parallel projections," *Medical Physics*, vol. 42, no. 2, pp. 831–845, 2015.

[12] S. Helgason, "The radon transform on euclidean spaces, compact two-point homogeneous spaces and grassmann manifolds," *Acta Mathematica*, vol. 113, no. 1, pp. 153–180, 1965.

[13] D. Ludwig, "The radon transform on euclidean space," *Communications on Pure and Applied Mathematics*, vol. 19, no. 1, pp. 49–81, 1966.

[14] S. R. Deans, *The Radon transform and some of its applications*. Courier Corporation, 2007.

[15] A. K. Louis, "Approximation of the radon transform from samples in limited range," in *Mathematical Aspects of Computerized Tomography*. Springer, 1981, pp. 127–139.

[16] A. S. Willsky and J. L. Prince, "Constrained sinogram restoration for limited-angle tomography," *Optical Engineering*, vol. 29, no. 5, pp. 535–544, 1990.

[17] H. Kudo and T. Saito, "Sinogram recovery with the method of convex projections for limited-data reconstruction in computed tomography," *Journal of the Optical Society of America A*, vol. 8, no. 7, pp. 1148–1160, 1991.

[18] G. B. Arfken and H. J. Weber, *Mathematical methods for physicists international student edition*. Academic press, 2005.

[19] R. Tibshirani, "Regression shrinkage and selection via the lasso," *Journal of the Royal Statistical Society. Series B (Methodological)*, pp. 267–288, 1996.

[20] I. Daubechies, M. Defrise, and C. De Mol, "An iterative thresholding algorithm for linear inverse problems with a sparsity constraint," *Communications on pure and applied mathematics*, vol. 57, no. 11, pp. 1413–1457, 2004.

[21] C. Tomasi and R. Manduchi, "Bilateral filtering for gray and color images," in *Computer Vision, 1998. Sixth International Conference on*. IEEE, 1998, pp. 839–846.

[22] A. Maier, H. Hofmann, M. Berger, P. Fischer, C. Schwemmer, H. Wu, K. Müller, J. Hornegger, J. Choi, C. Riess, A. Keil, and R. Fahrig, "CONRAD - a software framework for cone-beam imaging in radiology," *Medical Physics*, vol. 40, no. 11, p. 111914, 2013.